JMEPEG (2012) 21:191–196
DOI: 10.1007/s11665-011-9871-x

1059-9495/$19.00

Development of Processing Map for 7075 Al/20% SiC_p Composite

M. Rajamuthamilselvan and S. Ramanathan

(Submitted April 28, 2010; in revised form January 28, 2011)

The hot deformation behavior and microstructure evolution of 7075 Al/20% SiC_p composite have been studied using the processing map. Compression tests were carried out in the temperature range of 300-500 °C and at the strain rate range of 0.001-1.0 s^{-1}. The stable and unstable regions in the map were verified with the microstructural observations of the deformed compression specimens. The "stable" regions, i.e., dynamic recrystallization and "unstable" regions such as debonding of SiC particles, matrix crack, and adiabatic shear band formation were identified from the processing map and compared with the reported microstructural observations of the deformed compression specimens. The optimum hot working conditions for this composite were identified.

Keywords hot workability, metal-matrix composites, processing map

1. Introduction

Silicon-carbide particulate reinforced aluminum matrix composites (SiC_p/Al) have been well developed over the past few decades, owing to their excellent properties such as light weight, high elastic modulus, wear resistance, and low thermal expansion coefficient. Thus, the SiC_p/Al composites are expected to have many applications in aerospace, automobile, and electronic industries (Ref 1). The SiC_p/Al composites prepared by the general fabricating methods, such as powder metallurgy (PM), squeeze casting pressure, or pressureless infiltration and spray forming, tend to be slack and porous, which leads to the low ductility of such composites and prevents their applications (Ref 2). Thus the plastic processing, such as hot extrusion, is needed to improve their shaping/forming properties through refining the microstructures of the composites (Ref 3). Furthermore, the SiC_p/Al interface is another factor influencing the mechanical properties of the composites. The solid-liquid method to fabricate SiC_p/Al composites at high temperature often leads to brittleness and the interfacial reaction product Al_4C_3 is considered detrimental to the mechanical properties especially ductility and fracture strength of SiC_p/Al composites (Ref 4, 5).

Discontinuously reinforced Al composites have emerged as a well-defined class of advanced materials. These composites are aluminum-based materials reinforced by particles, whiskers, or short fibers. They merit attention because of their desirable properties like low density, high specific stiffness, reduced coefficient of thermal expansion, and increased fatigue resistance, along with the availability of comparatively low cost, high volume production methods. Compared to continuously reinforced composites, Al composites have the advantage of being amenable to conventional metal working operations such as extrusion, rolling, and forging (Ref 6). However, the standard hot working parameters for conventional matrix alloys cannot be directly adopted for these composites owing to the presence of hard ceramic reinforcements, which significantly affects their hot working characteristics. Hot workability is concerned with the extent to which a material plastically deforms during shaping at high temperatures without the occurrence of flow localization or fracture.

1.1 Development of Processing Map

One of the requirements for process modeling is the knowledge of the material flow behavior for defining deformation processing maps that delineate "safe" and "nonsafe" hot working conditions. These maps show the processing spaces. On the plot of temperature and strain rate, the processing conditions for stable and unstable deformation are marked. A processing map obtained by superimposing the instability map on the power dissipation map. It shows the power dissipation values for the material and the iso-efficiency contours are also plotted. The efficiency represents the relative rate of entropy production during hot deformation and characterizes the dissipative microstructure under different temperature and strain rate conditions. The input to generate a processing map is the experimental data of flow stress (σ) as a function of temperature (T), strain rate ($\dot{\varepsilon}$) and strain (ε). As the map generated will be only as good as the input data, it is important to use the accurate, reliable, and yet simple experimental technique for generating them.

In dynamic material model, the work piece under hot working conditions is considered to be a dissipater of power. The deformation behavior of any metallic material is governed by the internal constitution of the material and the rate of strain hardening. The strength of materials increases with increase in

M. Rajamuthamilselvan and **S. Ramanathan**, Department of Manufacturing Engineering, Annamalai University, Annamalai Nagar, TamilNadu 608002, India. Contact e-mail: rajanarmi@yahoo.co.in.

the plastic strain rate. The rate sensitive flow behavior is given by power law (Ref 7, 8).

$$\sigma = K\dot{\varepsilon}^m \quad \text{(Eq 1)}$$

$$m = \frac{\partial \log \sigma}{\partial \log \dot{\varepsilon}}|\varepsilon, T \quad \text{(Eq 2)}$$

where K is a parameter that depends upon structure of the material and temperature, m is the strain rate sensitivity, σ is the flow stress, $\dot{\varepsilon}$ is the strain rate, ε is strain, and T is the temperature. The value of m is determined by a variant of the Eq 1 given at a constant strain and temperature.

The deformation behavior of composites is influenced by the complexity of the dynamic microstructural processes. The deformation process is accompanied by two power dissipation routes (1) the power required to bring in microstructural changes in the work piece and (2) the dissipation in heat generation during deformation. For an ideal plastic flow, the flow stress is proportional to the strain rate at any strain and temperature. The efficiency is defined as the ratio of the heat dissipated in the microstructural changes and the maximum dissipation possible. The efficiency (η) of deformation is thus given by (Ref 6, 7)

$$\eta = \frac{2m}{m+1} \quad \text{(Eq 3)}$$

"m" is a function of deformation temperature and strain rate. The iso-efficiency contour plot on the temperature-strain rate field constitutes the processing map. Several domains can be identified in the map based on the η contours (i.e., power dissipation characteristics), each of them representing a dominant deformation mechanism. The peak efficiency condition of the domain corresponds to the optimum deformation condition. In addition to the η contours, the instability criterion given by the following Eq 4 (Ref 7):

$$\xi(\dot{\varepsilon}) = \frac{\delta \ln(m/(m+1))}{\delta \ln \dot{\varepsilon}} + m < 0 \quad \text{(Eq 4)}$$

is applied to delineate the temperature strain rate regimes of flow instability on the processing map.

The purpose of this investigation is to study the hot deformation behavior of 7075 aluminum alloy reinforced with 20% of SiC_p using the processing map technique and to establish the safe and unsafe domains. The domains are validated through microstructural observations.

2. Experimental Studies

Stir casting technique was used to fabricate 7075 Aluminum alloy (composition in wt.% Cu 1.66, Mg 2.10, Si 0.14, Mn 0.21, Fe 0.40, Cr 0.18, Zn 5.67, Ti 0.01, and rest Al) reinforced with 20% volume fraction of silicon carbide composites with an average size of 20 μm. The aluminum alloy was melted using an electric furnace. Preheated SiC_p (250 °C) was added to the melt and mixed by using a rotatory impeller in Argon environment and the melt was poured in a permanent mold. The cast billets were kept at the temperature of 400 °C for 30 min and hot extruded. The cylindrical specimens with the dimension of 10 mm in diameter and 10 mm in height were machined from the extruded rods.

The hot compression tests (Ref 9) were performed on a 10 ton servo controlled universal testing machine for different strains (0.1-0.5), strain rates (0.001-1.0 s^{-1}) and temperatures (300-500 °C). The temperature of the specimens was monitored with the aid of a chromel/alumel thermocouple embedded in a 0.5 mm hole drilled half the height of the specimens as stated by Siva (Ref 10) and Prasad and Rao (Ref 8). The thermocouple was also used for measuring the adiabatic temperature rises in the specimen during deformation. The specimens were effectively lubricated with graphite and deformed to a true strain of 0.5. After compression testing, the specimens were immediately quenched in water and the cross section was examined for microstructure. The specimens were deformed to half of the original height. Deformed specimens were sectioned along the direction parallel to the compression axis and the exposed surface was prepared for metallographic examination. The specimens were then etched with Keller's solution. The microstructures of the specimens were obtained through Versamet 2.0 optical microscope with Clemex vision Image Analyzer and the mechanism of deformation was studied. Using the flow stress data, power dissipation efficiency and flow instability were evaluated for different strain rates, temperatures at the constant strain of 0.5. The processing maps were developed for 0.5 strain for the 7075Al/20% SiC_p composite.

3. Results and Discussion

The hot compression tests were performed on 7075 aluminum alloy reinforced with 20% of SiC_p composites with temperature range of 300-500 °C and strain rate range of 0.001-1.0 s^{-1} in different strains (0.1-0.5). Flow stress data have been obtained from the load-stroke data.

The flow stress of a material is influenced by the factors unrelated to the deformation process such as chemical composition, metallurgical structure, phases, grain size, deformation, prior strain history, and factors explicitly related to the deformation process such as temperature of deformation by power expression of the form in Eq 3 (Ref 8), degree of deformation or strain and the rate of deformation or strain rate. The input to generate a processing map is the experimental data of flow stress as a function of temperature, strain rate, and strain. As the map generated will be only as good as the input data, it is important to use accurate, reliable, and simple experimental technique for generating them. In general, the material starts "flowing" or deforming plastically when the applied stress (in uniaxial tension without necking or in uniaxial compression without bulging) reaches the value of the flow stress.

3.1 Interpretation from Flow Stress-Flow Strain Curves

Two main processes govern the flow stress behavior of a metal matrix composite: the transfer of load from the ductile matrix to the hard particles and the microstructural transformations such as recrystallization or damage phenomena. In damage process, the composite can present decohesion at the interfaces of matrix-particles or clusters of several particles. When the material is able to dissipate the provided power through the load transfer or through phase transformations, it does not reach high levels of damage (Ref 11).

A number of stress-strain relationships suggested have been tested with respect to their ability to approximate experimental data. In particular, various methodologies to express flow characteristics at high temperatures in microscopic aspects have been proposed and evaluated by many researchers (Ref 12, 13).

The flow stress data were generated covering the temperature range of 300-500 °C and strain rate range 0.001-1.0 s^{-1} from the compression tests. The values of the efficiency parameter (η) and the strain rate sensitivity parameter (m) to use the instability condition (Ref 14) were determined from the flow stress test data of the material.

The flow curves obtained for 7075Al/20% SiC_p composites deformed in compression at 400 °C at different strain rates ranging from 0.001 to 1.0 s^{-1} were presented in Fig. 1. The flow stress is significantly low at lower strain rates whereas the work hardening rate is relatively high. Hence, the flow stresses increase with decreasing temperature and increasing strain rate.

At lower strain, it is adiabatic. The increase in strength is attributed to dispersive hardening effect of the SiC particles. The flow stress-strain curves exhibit flow softening at higher strain rates. The rise in temperature leads to decrease in work hardening rate (Ref 15). The flow curves for different temperatures at the constant strain rate of 0.1 s^{-1} are shown in Fig. 2. At lower temperature, the strain hardening is high and the steady state reached between 300 and 400 °C. The matrix around the SiC particles has increased dislocation density. The true stress increases to a peak value and then falls down, which suggests flow softening between 450 and 500 °C. The high dislocation density regions restrict the plastic flow and contribute to the strengthening and strain hardening (Ref 15). As the temperature increases, the strengthening effect of SiC particles is considerably diminished.

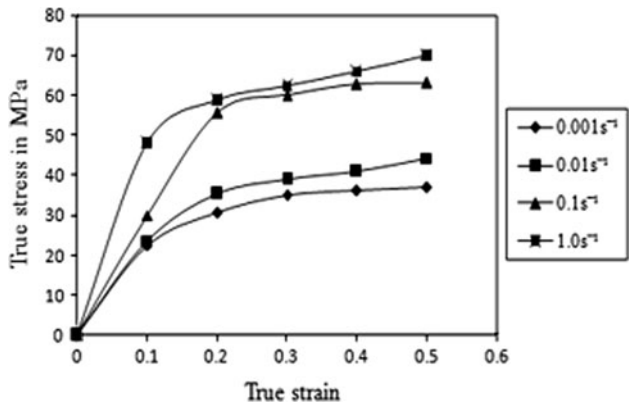

Fig. 1 The flow curves for different strain rates at constant temperature 400 °C

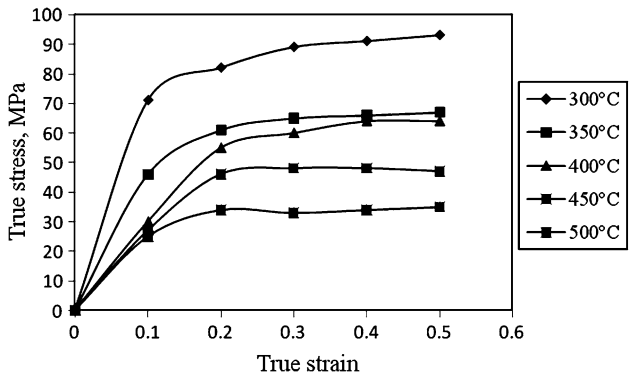

Fig. 2 The flow curves for different temperatures at constant strain rate 0.1 s^{-1}

3.2 Microstructure Analysis

The properties of a metal are strongly influenced by its microstructural features like the grain size and the grain/subgrain orientation/mis-orientation. The mechanism of microstructure evolution during thermo-mechanical processing includes strain hardening, recrystallization, and grain growth. The stored energy was established early as one of the important driving forces behind recrystallization. Recrystallization is the further restoration process wherein new dislocation free grains are formed within the deformed microstructure. Recrystallization may also take place during deformation at elevated temperatures and this is termed as the dynamic recrystallization.

The driving force for recrystallization is known to be supplied by the stored energy toward the nucleation of new grains both within the grain and at the grain boundaries. A general form of the dynamic recrystallization recovery function with this driving force was given in terms of the deformation resistance (Ref 16). Dynamic recrystallization (DRX) helps to soften the material and the recovery mechanism leading to DRX is likely to be strain rate-dependent lattice self diffusion (Ref 17). DRX is a beneficial process in hot deformation as it gives stable flow and good workability to the materials by simultaneously softening. However, it changes the microstructure (Ref 18). At sufficiently high temperature, DRX is initiated at some critical stress attained at critical strain. As a flow-softening phenomenon, DRX leads to a decrease in flow stress with increasing strain. It does not occur immediately after the critical stress has attained. Beyond this critical point, the stress continues to increase until the softening due to the progress of DRX that balances the continuing strain hardening in the uncrystallized parts of the material. This balance is manifested by the peak stress attained at the strain. The major experimental difficulty in detecting the onset of DRX is that the attainment of the critical stress does not reveal itself in the flow curve. Although, the flow stress peaks in constant strain rate deformation are good indications that DRX is well underway; they do not provide information about the onset of DRX.

The processing map at the strain of 0.5 is shown in Fig. 3. This strain may be considered large enough to cause steady state flow. The map exhibits one domain, occurs in the temperature range of 360-430 °C and at strain rate range of 0.04-0.2 s^{-1} with a peak efficiency of about 40% occurring at 400 °C and 0.1 s^{-1}. Initial microstructure of the composite is shown in Fig. 4. Microstructure analysis reveals that the initial microstructure was replaced (Fig. 5) by recrystallized structure. This domain represents the region of possible dynamic recrystallization. The microstructure as given in Fig. 5 shows that DRX occurred at this temperature. Grain elongation is obtained at the temperature of 400 °C at the strain rate of 0.01 s^{-1}, which is shown in Fig. 6. The map did not exhibit any flow instability regime that could restrict the hot workability.

The processing and instability map of the studied material is shown in Fig. 3. Typical material instabilities are void formation, adiabatic shear bands, particle debonding, and matrix cracking. The flow instability occurs in three different zones. The instability occurred at higher strain rates between 0.1 and

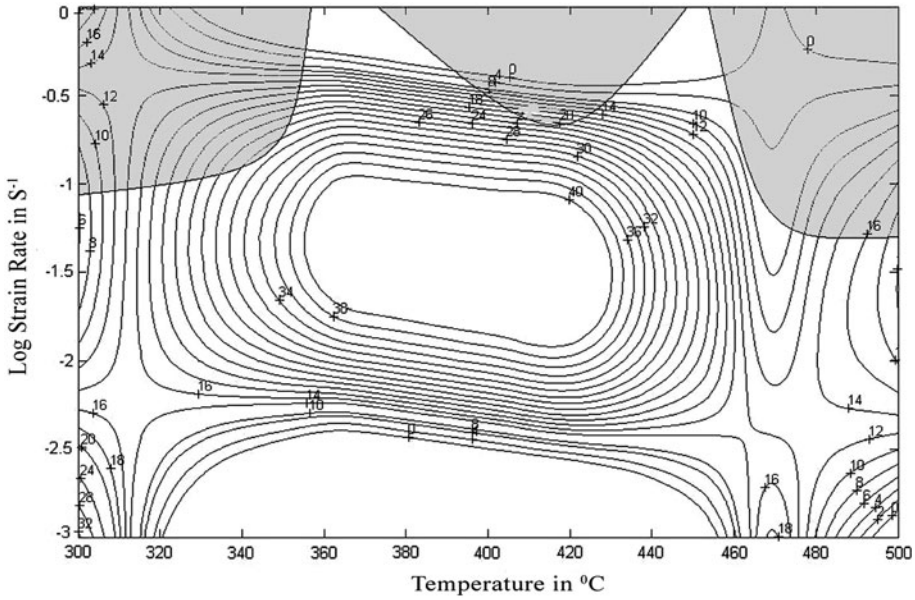

Fig. 3 Processing map for 7075Al/20% SiC_p composites at 0.5 strain

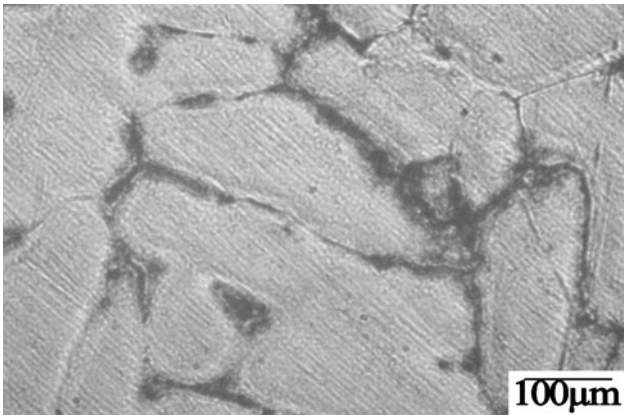

Fig. 4 Initial microstructure of composite

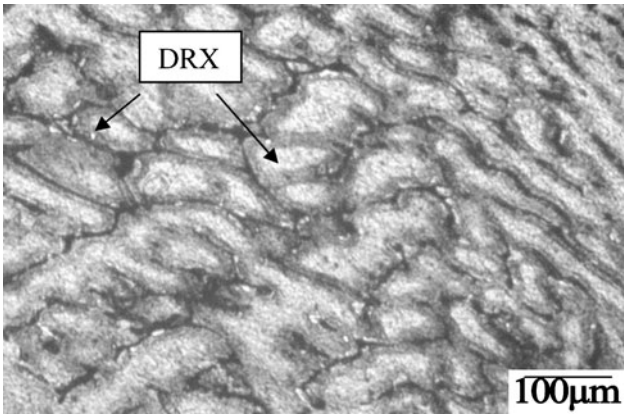

Fig. 5 Dynamic recrystallization at 400 °C at a strain rate of 0.1 s^{-1}

1.0 s^{-1} and at three different temperature ranges of 300-350, 380-450, and 460-500 °C. The calculation of the dissipation efficiency leads to the conclusion that the efficiency (η)

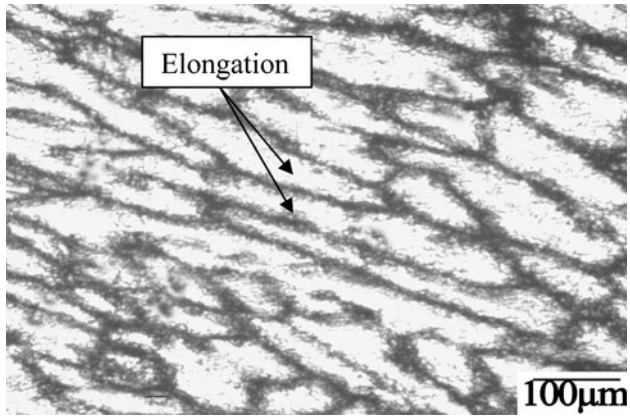

Fig. 6 Elongation at 400 °C and a strain rate of 0.01 s^{-1}

increases with increasing temperature in the strain rate regime investigated. The voids are generated by cracking of the reinforcement particles. Almost all particles near the surface are cracked and accompanied by voids with a few interior particles cracked. The difference in thermal expansion coefficients between the matrix and SiC particles necessitates, the generation of dislocations in matrix close to SiC_p to accommodate the thermal strain (Ref 19). Many fractured particles and voids around the reinforcing phases were observed at 350 °C at in the strain rates of 1.0 s^{-1}. In these deformation regimes, the matrix is not so ductile to dissipate the stress but transfers a large part of the force to the particles with the consequence of big void formation as shown in Fig. 7.

An adiabatic shear band in the microstructure indicates that the deformation is not uniform. Figure 3 shows an unstable domain at higher strain rates above 1.0 s^{-1} because of the possible occurrence of adiabatic shear bands or localized plastic flow. These predictions are further validated by the microstructural observations on the deformed specimens. Figure 8 shows the micrograph of the specimen deformed at 300 °C and 1.0 s^{-1}, where adiabatic shear bands can be observed at an

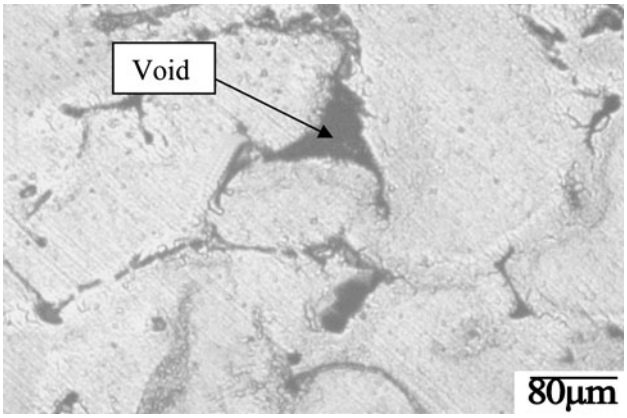

Fig. 7 Voids formation at 350 °C and at strain rates of 1.0 s^{-1}

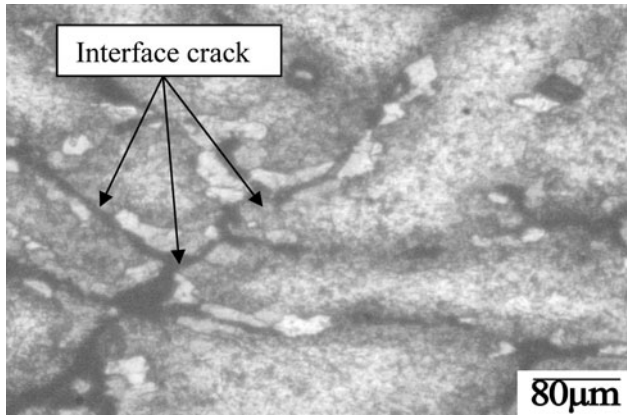

Fig. 9 Interface crack at 500 °C and at a strain rate of 1.0 s^{-1}

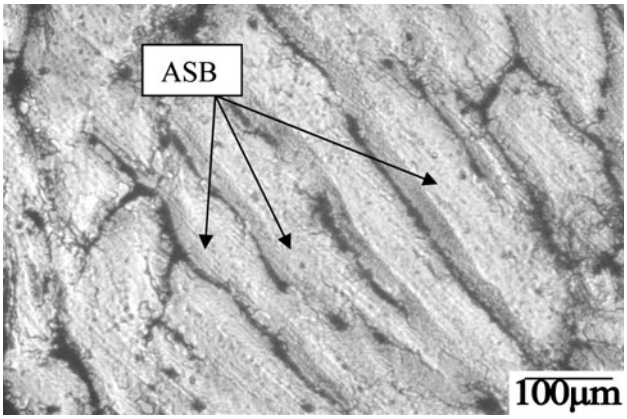

Fig. 8 Shear band formation at 300 °C and at a strain rate of 1.0 s^{-1}

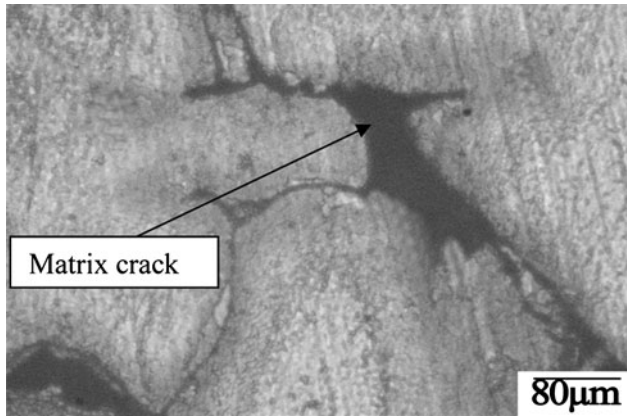

Fig.10 Matrix crack observed at 500 °C and at a strain rate of 1.0 s^{-1}

angle of about 45° to the compressive axis. At higher strain rates, the deformation is adiabatic. The heat generated during hot working was not conducted away due to insufficient time and low thermal conductivity, indicating highly localized flow along the maximum shear stress plane (Ref 20).

If hard particles are present in a soft matrix, deformation causes the interface to crack and deboned as the matrix undergoes plastic flow while the particles do not deform. The interfacial failure observed in the current composite is different from the simple interfacial debonding that the SiC particles are pulled out from metal matrix with clear surfaces (Ref 21). These differences might be explained by the high strength of metal matrix and SiC_p/Al interfaces in the composites produced in the current experiment. Figure 9 shows that the bonding between the particles and the matrix is weak. It is evident that the particle debonding is due to interfacial failure. Aluminum matrix is seen sticking to the surface of the SiC_p. A gap between the matrix and the particle is also seen. This feature is observed at 400 °C in 1.0 s^{-1}.

The elongation increases with increasing temperature, even up to temperatures higher than its liquid phase temperature for the super plastic aluminum matrix composites. High elongation results from the presence of excessive liquid phase at grain/interface boundaries. In addition to grain boundary sliding, extensive interfacial sliding also takes place. The presence of SiC particles in aluminum matrix when deformed causes the interface to crack and de-bond of SiC particles occurs at higher temperatures (Ref 22). Matrix crack observed at 1.0 s^{-1} and 500 °C is shown in Fig. 10 due to wedge cracking.

4. Conclusions

The hot deformation behavior of 7075 Al/20% SiC_p composite has been studied by employing hot compression tests in the temperature and strain ranges of 300-500 °C and 0.001-1.0 s^{-1}, respectively.

Dynamic recrystallization occurs in the temperature range of 360-430 °C and strain rate range of 0.04-0.2 s^{-1}. The optimum processing parameters for hot working of 7075 Al/20% SiC_p composite are 400 °C and 0.1 s^{-1} having efficiency of 40%, are identified. At higher strain rate, the material exhibits flow instability such as adiabatic shear band, debonding, and matrix cracking. These temperatures and strain rates should be avoided in processing the material.

Acknowledgments

The authors are grateful to The Department of Manufacturing Engineering, Annamalai University, Tamilnadu, India for the support for fabrication and testing of the composite.

References

1. C. Badini, G.M. La Vecchia, P. Fino, and T. Valente, Forging of 2124/SiCp Composites: Preliminary Studies of the Effect on Microstructure and Strength, *J. Mater. Process. Technol.*, 2000, **116**, p 289–297
2. H.S. Lee, J.S. Yeo, S.H. Hong, D.J. Yoon, and K.H. Na, The Fabrication Process and Mechanical Properties of SiCP/Al-Si Metal Matrix Composites for Automobile Air-Conditioner Compressor Pistons, *J. Mater. Process. Technol.*, 2001, **113**, p 202–208
3. H.K. Seok, J.C. Lee, and H.I. Lee, Extrusion of Spray-Formed Al-25Si-X Composites and their Evaluation, *J. Mater. Process. Technol.*, 2005, **160**, p 354–360
4. L.M. Tham, M. Gupta, and L. Cheng, Effect of Limited Matrix-Reinforcement Interfacial Reaction on Enhancing the Mechanical Properties of Aluminium-Silicon Carbide Composites, *Acta Mater.*, 2001, **49**, p 3243–3253
5. L.M. Tham, M. Gupta, and L. Cheng, Predicting the Failure Strains of Al/SiC Composites with Reacted Matrix-Reinforcement Interfaces, *Mater. Sci. Eng. A*, 2003, **354**, p 369–376
6. S.V.S. Narayana Murty, B. Nageswara Rao, and B.P. Kashyap, On the Hot Working Characteristics of 2014 Al–20 vol% Al2O3 Metal Matrix Composite, *J. Mater. Process. Technol.*, 2005, **166**, p 279–285
7. S.V.S. Narayana Murty, B. Nageswara Rao, and B.P. Kashyap, On the Hot Working Characteristics of 6061Al-SiC and 6061-Al_2O_3 Particulate Reinforced Metal Matrix Composites, *Composites Sci. and Tech.*, 2003, **63**, p 119–135
8. Y.V.R.K. Prasad and K.P. Rao, Processing Maps and Rate Controlling Mechanisms of Hot Deformation of Electrolytic Tough Pitch Copper in the Temperature Range 300–950°C, *Mater. Sci. Eng. A*, 2005, **391**, p 141–150
9. Y.C. Lin, M.-S. Chen, and J. Zhong, Prediction of 42CrMo Steel Flow Stress at High Temperature and Strain Rate, *Mech. Res. Commun.*, 2008, **35**(3), p 142–150
10. O. Siva, Characteristics of Super Plasticity Domain in the Processing Map for Hot Working of As Cast Mg-11.5 Li-1.5 Al Alloy, *Mater. Sci. Eng. A*, 2002, **323**, p 270–277
11. Y.V.R.K. Prasad and K.P. Rao, Processing Maps and Rate Controlling Mechanisms of Hot Deformation of Electrolytic Tough Pitch Copper in the Temperature Range 300–950°C, *Mater. Sci. Eng. A*, 2005, **391**, p 141–150
12. S. Spigarelli, E. Cerri, P. Cavaliere, and E. Evangelista, An analysis of Hot Formability of the 6061 + 20% Al_2O_3 Composite by Means of Different Stability Criteria, *Mater. Sci. Eng. A*, 2002, **327**, p 144–154
13. S. Serajzadeh and A.K. Taheri, An Investigation on the Effect of Carbon and Silicon on Flow Behavior of Steel, *Mater. Des.*, 2002, **23**, p 271–276
14. S. Serajzadeh and A.K. Taheri, Prediction of Flow Stress at Hot Working Condition, *Mech. Res. Commun.*, 2003, **30**, p 87–93
15. T. Seshacharyulu, S.C. Medeiros, J.T. Morgan, J.C. Malas, W.G. Frazier, and Y.V.R.K. Prasad, Hot Deformation and Microstructural Damage Mechanisms in Extra Low Interstitial (ELI) Grade Ti-6Al-4V, *Mater. Sci. Eng. A*, 2000, **279**, p 289–299
16. P. Cavaliere, E. Cerri, and P. Leo, Hot Deformation and Processing Maps of a Particulate Reinforced 2618/Al2O3/20p Metal Matrix Composite, *Compos. Sci. Technol.*, 2004, **64**, p 1287–1291
17. S. Ganapathysubramanian and N. Zabaras, Deformation Process Design for Control of Microstructure in the Presence of Dynamic Recrystallization and Grain Growth Mechanisms, *Int. J. Solids Struct.*, 2004, **41**, p 2011–2037
18. K.P. Rao, Y.V.R.K. Prasad, N. Hort, and K.U. Kainer, Hot Workability Characteristics of Cast and Homogenized Mg–3Sn–1Ca Alloy, *J. Mater. Process. Technol.*, 2008, **201**, p 359–363
19. W.D. Zeng, Y.G. Zhou, J. Zhou, H.Q. Yu, X.M. Zhang, and B. Xu, Recent Development of Processing Map Theory, *Rare Met. Mater. Eng.*, 2006, **35**, p 673–677
20. P. Cavaliere and E. Evangelist, Isothermal Forging of Metal Matrix Composites: Recrystallization Behaviour by Means of Deformation Efficiency, *Compos. Sci. Technol.*, 2006, **66**, p 357–362
21. S.H. Nie and C.A. Basaran, A Micromechanical Model for Effective Elastic Properties of Particulate Composites with Imperfect Interfacial Bonds, *Int. J. Solids Struct.*, 2005, **42**, p 4179–4191
22. A.B. Li, L.J. Huang, Q.Y. Meng, L. Geng, and X.P. Cui, Hot Working of Ti–6Al–3Mo–2Zr–0.3Si Alloy with Lamellar $\alpha + \beta$ Starting Structure Using Processing Map, *Mater. Des.*, 2009, **30**, p 1625–1631